Multiple source analysis from InSAR data and new insights into fault activation and stress transfer: The 2005 Zarand, Iran, earthquake

Zeinab Golshadi[1], Mehdi Rezapour[1], Simone Atzori[2] and Stefano Salvi[2]
[1]*Institute of Geophysics, University of Tehran, Tehran, Iran.*
[2]*Istituto Nazionale di Geofisica e Vulcanologia, Rome, Italy*

ABSTRACT

We have reinterpreted the causative fault parameters of the 2005 Zarand earthquake in the light of a new imagery study using Interferometric Synthetic Aperture Radar (InSAR). By conducting a joint inversion of two InSAR datasets, we can characterize the rupture as it relates to complex local structures. At first, the mainshock ruptured a nearly pure thrust fault, dipping ~65° NNW in the basement below the southeastern area of Zarand. Two more fault segments were subsequently activated: an oblique-normal fault segment parallel to the first segment, dipping 61° to the south, and a normal-oblique fault segment at the eastern termination of the rupture zone. The first fault segment ruptured the surface, while slip along the other two segments was confined to the lower sedimentary strata. The stress changes induced by the main fault segment that affected the other two segments were also measured, and showed progressive failure along the fault segments.

Keywords: InSAR, Zarand earthquake, multiple source, stress transfer.

INTRODUCTION

On February 22, 2005 at 02:25 UTC (05:55 local time), the Mw 6.4 Zarand earthquake occurred in a seismically active area of the Kerman province, southeastern Iran (Figure 1). This earthquake occurred on previously recognized faults in a region with a high attenuation rate (Ma'hood and Hamzehloo, 2009), which limited the radius of the highly damaged area to 16 km from the epicenter (Hoseini Hashemi et al., 2005).

Several source mechanisms (Table 1), have been calculated for this earthquake using different techniques. The Global Centroid Moment Tensor (GCMT) solution obtained by Harvard group and the U.S. Geological Survey (USGS) is a fault-plane solution that is consistent with nearly pure thrust-slip motion, but the USGS solution prefers a smaller seismic moment release. Talebian et al. (2006) also studied the earthquake source characteristics using body wave inversion, field observations and Interferometric Synthetic Aperture Radar (InSAR) data. They also mapped an apparent surface rupture that stretched for approximately 13 km. Based on an inversion of near-field strong motion data, Rouhollahi et al. (2012) introduced a fault slip model that suggest a bilateral rupture was produced by the earthquake .

In this study, we analyze the complexity of the source of the Zarand 2005 earthquake that has not been presented by previous studies. Through inversion modeling of displacement data (measured using InSAR data), we can identify multiple earthquake sources and calculate their geometries, kinematics, and slip distributions. We also try to reconcile the convergent tectonics of the region and the segmented strike-slip Kuhbanan fault system with the complex source configuration determined in the model. We also calculate the Coulomb stress changes on the seismic ruptures and analyze their possible interactions.

BODY OF THE DOCUMENT (Methodology & Data,…)

We analyzed the displacement maps, obtained from the InSAR technique (Massonnet et al., 1993), using images acquired from ENVISAT, a C-band radar satellite from the European Space Agency, on both ascending and descending tracks. We generated interferograms from two pairs of images with 0.028 altitudes of ambiguity, covering an interval 35 days that included the earthquake.

We started modeling the InSAR data by re-sampling the unwrapped interferograms. Then, co-

seismic displacement modeling was conducted using a consolidated two-step approach via Non-Linear inversion to solve for the co-seismic displacements on a rectangular dislocation with fault parameters, and Linear inversion to solve for the slip distribution along the fault (Atzori et al., 2009). In both steps, the underlying model was a rectangular dislocation in a homogeneous and elastic half-space (Okada, 1985). Both inversions accounted for topographic compensation, according to Williams and Wadge (1998).

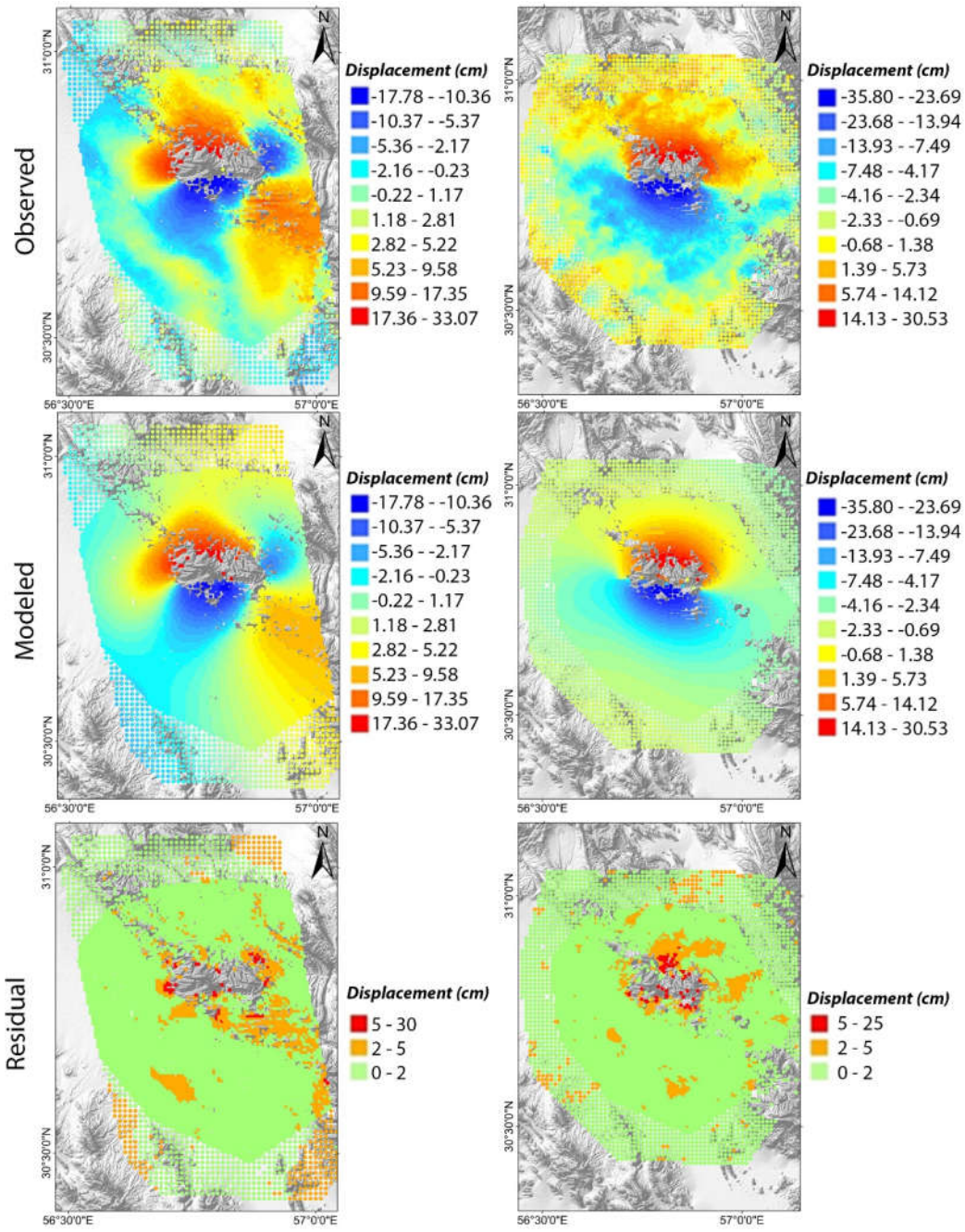

Figure 1. Results of our best model derived from joint linear least-square inversions for ascending (left) and descending (right) observations. Observed, modeled, and residual displacement maps for the two unwrapped co-seismic interferograms obtained for the 2005 Zarand earthquake. Color legends are scaled according to the minimum/maximum value of the observed and modeled maps for the two datasets, separately, while the same color scheme is used for the residual maps..

Table1. Modeled fault parameters for the Zarand earthquake. Depths are to the top of the fault from the surface, and coordinates indicate the center of the fault trace..

Fault segment	Width (m)	Length (m)	Depth (m)	Strike (°)	Dip (°)	Longitude	Latitude	Rake (°)	Slip (m)	Moment (Nm)	Focal mechanism
1	16000	20000	0	277	65	56.79	30.81	105	1.61	4.70E+018	
2	6000	6000	0	96	61.54	56.76	30.80	-151.6	0.94	8.55E+017	
3	6000	7000	0	164	72.65	56.85	30.82	-111.28	1.02	4.10E+017	
Overall										5.97E+018	

CONCLUSION(S)

The February 22, 2005 Mw 6.4 Zarand earthquake involved a complex series of fault segments: a nearly pure thrust fault, dipping ~65° NNW, an oblique-normal fault segment parallel to the first with a 61° southward dip, and a normal-oblique slip fault at the eastern termination of the rupture zone .

The causative fault segments determined by this study were compared to structures on geological maps, which demonstrated the role of pre-existing local structures in propagating stress and producing a larger earthquake.

In this case, the strain release comprised multiple sub-events that took place on a complex network of fault segments. Of particular interest is the observation that there was a stress change induced by the main fault on two other segments (based on the ΔCFF). We show that static stress variations consistently favored the advance of failure along fault segments, and thus this area can be identified as an active zone.

REFERENCES

Ambraseys, N. N. and Melville, C. P., 1982. A History of Persian Earthquakes. Cambridge Univ. Press .

Atzori, S., Hunstad, I., Chini, M., Salvi, S., Tolomei, C., Bignami, C., … Boschi, E., 2009. Finite fault inversion of DInSAR coseismic displacement of the 2009 L'Aquila earthquake (central Italy). Geophysical Research Letters, 36(15), L15305, doi:10.1029/2009GL039293 .

Atzori, S., Manunta, M., Fornaro, G., Ganas, A. and Salvi, S., 2008. Postseismic displacement of the 1999 Athens earthquake retrieved by the Differential Interferometry by Synthetic Aperture Radar time series. Journal of Geophysical Research: Solid Earth, 113(9), B09309, doi:10.1029/2007JB005504 .

Berberian, M., 2014. Earthquakes and coseismic surface faulting on the Iranian Plateau : a historical, social and physical approach. Elsevier, Amsterdam, ISBN 978-0-444-63292-0.

Costantini, T. M., 1998. A novel phase unwrapping method based on network programming. IEEE Transactions on Geoscience and Remote Sensing, 36(3), 813–821 .

Davoudzadeh, M. and Schmidt, K., 1984. A Review of the Mesozoic Paleogeography and Paleotectonic Evolution of Iran. Neues Jahrbuch Für Geologie Und Paläontologie - Abhandlungen, 168(2–3), 182–207.

Engdahl, E. R., van der Hilst, R. and Buland, R., 1998. Global teleseismic earthquake relocation with improved travel times and procedures for depth determination. Bulletin of the

Seismological Society of America, 88(3), 722–743.
Farr, T. G., Rosen, P. A., Caro, E., Crippen, R., Duren, R., Hensley, S., … Alsdorf, D., 2007. The Shuttle Radar Topography Mission. Reviews of Geophysics, 45(2), RG2004, doi:10.1029/2005RG000183 .
Funning, G. J., Parsons, B., Wright, T. J., Jackson, J. A. and Fielding, E. J., 2005. Surface displacements and source parameters of the 2003 Bam (Iran) earthquake from Envisat advanced synthetic aperture radar imagery. Journal of Geophysical Research: Solid Earth, 110(9), B09406, doi:10.1029/2004JB003338 .
Goldstein, R. M. and Werner, C. L., 1998. Radar interferogram filtering for geophysical applications. Geophysical Research Letters, 25(21), 4035–4038 .
Hamedpour Darabi, M., Piper, J. A. D., Kheradmand, A., Rezaie, P. and Mortazavi, M., 2010. AMS study of the Dezou and Dahou series in the Kerman-Zarand region. Journal of the Earth and Space Physics, 36(1), 109–126.
Harris, R. A., 1998. Introduction to Special Section: Stress Triggers, Stress Shadows, and Implications for Seismic Hazard. Journal of Geophysical Research: Solid Earth, 103, 24347–24358 .
Hessami, K., Jamali, F. and Tabasi, H., 2003. Map of Major active faults of Iran at 1:2500000. Ministry of Science, Research and Technology, International Institute of Earthquake Engineering and Seismology.
Hoseini Hashemi, B., Hamzeloo, H. and Davoudi, M., 2005. 2005 Zarand earthquake preliminary report. International Institute of Earthquake Engineering and Seismology.
Ma'hood, M. and Hamzehloo, H., 2009. Estimation of coda wave attenuation in East-Central Iran. Journal of Seismology, 13(1), 125–139 .
Marquardt, D. W., 1963. An Algorithm for Least-Squares Estimation of Nonlinear Parameters. Journal of the Society for Industrial and Applied Mathematics, 11(2), 431–441 .
Massonnet, D., Rossi, M., Carmona, C., Adragna, F., Peltzer, G., Feigl, K. and Rabaute, T., 1993. The displacement field of the Landers earthquake mapped by radar interferometry. Nature, 364(6433), 138–142 .
Okada, Y., 1985. Surface deformation due to shear and tensile faults in a half-space. Bulletin of the Seismological Society of America, 75(4), 1135–1154.
Pollastro, R. M., Persits, F. M. and Steinshouer, D. W., 1997. Maps showing geology, oil and gas fields, and geologic provinces of Iran. USGS Open-File Report, 97-470-G, https://doi.org/10.3133/ofr97470G
Rosen, P. A., Hensley, S., Peltzer, G. and Simons, M., 2004. Updated repeat orbit interferometry package released. Eos, 85(5), 47 pp.
Rouhollahi, R., Ghayamghamian, M. R., Yaminifard, F., Suhadolc, P. and Tatar, M., 2012. Source process and slip model of the 2005 Dahuiyeh-Zarand earthquake (Iran) using inversion of near-field strong motion data. Geophysical Journal International, 189(1), 669–680 .
Shafiei Bafti, A., Shahpasand-Zadeh, M., Iranmanesh, F., Tavakoli, F. and Shirzaii, M., 2007. Quaternary slip rate on the Kuh Banan strike-slip fault system, Southeast Iran, inferred from geomorphic features and geodetic measurements. European Geosciences Union 2007, Austria, Vienna, 9.
Talebian, M., Biggs, J., Bolourchi, M., Copley, A., Ghassemi, A., Ghorashi, M., … Saiidi, A., 2006. The Dahuiyeh (Zarand) earthquake of 2005 February 22 in central Iran: reactivation of an intramountain reverse fault. Geophysical Journal International, 164(1), 137–148 .
Vahdati Daneshmand, F., Mosavvari, F., Mahmoudi, M. H. and Ghasemi, A., 1995. Geology map of Zarand, Scale: 1:100000. Geological Survay of Iran, https://gsi.ir/fa/map/435
Vernant, P., Nilforoushan, F., Hatzfeld, D., Abbassi, M. R., Vigny, C., Masson, F., … Chéry, J., 2004. Present-day crustal deformation and plate kinematics in the Middle East constrained by GPS measurements in Iran and northern Oman. Geophysical Journal International, 157(1), 381–398 .
Walker, R. T., Talebian, M., Saiffori, S., Sloan, R. A., Rasheedi, A., MacBean, N. and Ghassemi, A., 2010. Active faulting, earthquakes, and restraining bend development near Kerman city in southeastern Iran. Journal of Structural Geology, 32(8), 1046–1060 .